

## COMPACT AND DIFFUSE DOUBLE LAYER INTERACTION IN UNSUPPORTED SYSTEM SMALL-SIGNAL RESPONSE \*

J. ROSS MACDONALD and DONALD R. FRANCESCHETTI

*Department of Physics and Astronomy, University of North Carolina, Chapel Hill, N.C. 27514 (U.S.A.)*

(Received 8th August 1978; in revised form 30th October 1978)

### ABSTRACT

Previous exact results for the small-signal impedance of an unsupported electrode/material/electrode system which include effects of the finite size of charge carriers are simplified and discussed. The material contains non-recombining charges of opposite sign with the positive one immobile and uniformly distributed. General boundary conditions which encompass the range from no electrode reaction to ohmic electrode behavior are employed. In the presence of an electrode reaction, the interaction of the compact and diffuse double layers leads to considerably more complexity in the equivalent circuit than might appear in simple treatments of the supported case, in which the diffuse double layer capacitance is neglected or the compact double layer and diffuse double layer capacitances are placed in series. Two different approximate equivalent circuits made up of frequency-independent elements are found which yield remarkable agreement with the exact results over the entire frequency range of interest. The first involves the ordinary approximate circuit (OAC) previously found in the absence of compact layer effects plus a series compact layer contribution involving a parallel resonant circuit with quality factor at resonance which may approach unity. Pseudo-inductance effects are found to be extremely significant in this representation. The second approximate equivalent circuit, simpler and almost as accurate as the first, has the same form as the original OAC but with its reaction element values altered by the presence of the compact layer. For non-Butler-Volmer electrode kinetics an upper limit is found for the experimentally determinable apparent reaction rate constant, a feature of practical importance for thin films or membranes. The response of thin films and membranes, including compact layer effects, can very readily be erroneously confused with pure bulk response, yielding entirely incorrect values for the geometrical capacitance and bulk resistance of the material.

### (1) INTRODUCTION

In recent papers [1–3], we derived and examined an exact expression for the small-signal response of a material with two species of charge carrier, one effectively immobile and uniformly distributed and the other, of opposite sign, free to move and react at two identical, plane parallel electrodes. Our treatment allowed for the possible presence of compact layers at the electrodes through the use of rather general, overpotential-dependent boundary conditions which could represent Chang-Jaffé (overpotential-independent, no compact layer), Butler-Volmer, or other electrode kinetics through an appropriate choice of

\* Work supported by U.S. National Science Foundation (Grant No. DMR 76-84187).

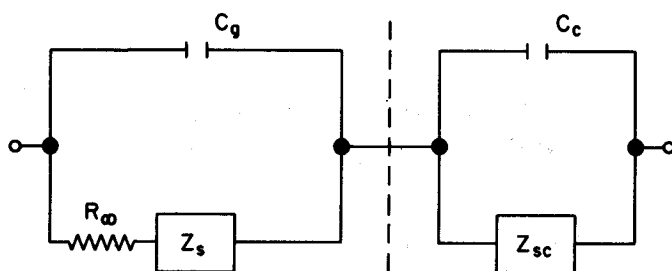


Fig. 1. Equivalent circuit for the exact impedance,  $Z_T$ , when compact layers are present. The impedance of the left circuit is  $Z_{CJ}$ , that of the right  $Z_{CL}$ , and  $Z_T = Z_{CJ} + Z_{CL}$ .

parameters. As in previous exact work on small-signal a.c. response [4] it was necessary to assume flat-band equilibrium conditions (the absence of intrinsic space-charge layers) in order to obtain a solution in closed form. Although the possible occurrence of specific adsorption was considered in our original discussion, for simplicity it will be excluded here.

In this work we consider the representation of small-signal response, including compact layer effects, by two approximate equivalent circuits composed of frequency-independent elements. The circuits are derived from the exact impedance expression presented earlier and in particular from the circuit representation given in Fig. 1, for which the components are defined below. The separation of the total impedance into two parts as depicted in the Figure is that which apparently leads to the most accurate approximate equivalent circuit composed solely of frequency independent elements, a representation sufficiently accurate that it may be used in data analysis in place of the exact result with negligible error. A second approximate circuit, of considerably simpler form, is then introduced and is shown to provide, in many cases, nearly as accurate a representation of the system response as the first approximate circuit. Expressions are given for the values of the elements of the second, simpler, circuit in terms of the elements of the first approximate circuit, which are defined with respect to the fundamental circuit parameters.

In Fig. 1, the right hand circuit involves a compact layer capacitance,  $C_C$ , and a parallel impedance  $Z_{SC}$ , also associated with compact layer effects.  $C_C$  has the usual Helmholtz model form and will here be considered as a parameter of known value. The exact impedance in the absence of compact layers (i.e.  $C_C = \infty$ ) is denoted  $Z_{CJ}$  and is represented by the portion of the circuit on the left hand side of the dashed line. Here  $C_g$  is the geometrical capacitance of the entire system excluding compact layer regions and  $R_\infty$  its high-frequency limiting resistance. Both quantities thus involve the length  $l$ , the distance between the electrodes minus the thickness of the two compact layers. All definitions not given herein may be found in the earlier work cited.

In the remainder of this work impedances and admittances will be normalized with  $R_\infty$ , so that  $Z_N \equiv Z/R_\infty$  and  $Y_N \equiv Z^{-1} \equiv YR_\infty$ ; capacitances normalized with  $C_g$ ,  $C_N \equiv C/C_g$ ; and frequency normalized with  $\tau_D^{-1}$ ,  $\Omega \equiv \omega\tau_D$ , where  $\tau_D \equiv R_\infty C_g$  is dielectric relaxation time of the material. Processes of most importance in the present context appear for  $\Omega < 100$ . Another impor-

tant quantity is the normalized half-length, which may be expressed either as  $M \equiv l/2L_D$  or as  $M_n \equiv l/2\sqrt{2}L_D \equiv l/2L_{Dn} \equiv M/\sqrt{2}$ , where  $L_D$  is the bulk Debye length for both carrier species mobile and  $L_{Dn} \equiv \sqrt{2}L_D$  is the Debye length for negative carriers alone mobile, the case we shall consider here.

## (II) ANALYSIS

In this Section, we shall derive the first of the two approximations to the exact solution and consider its associated equivalent circuit. The adequacy of the two approximations will be examined in detail in later Sections. In the present case of no specific adsorption, one finds that the exact expression for the normalized impedance involves the four frequency-independent dimensionless parameters  $M$ ,  $C_{CN}$ ,  $\rho_2$ , and  $\nu_2$ . Here  $\rho_2$  (previously denoted  $r_n/2$  or  $r_2/2$ ) is a normalized reaction rate parameter for negative mobile charges [4]; the normalized reaction resistance associated with it is  $R_{RN} \equiv \rho_2^{-1}$ ; and  $\nu_2$  (previously denoted  $\nu_n$ ) is a parameter which specifies the dependence of the rate of electrode reaction of the negative charges on the overpotential. There is no dependence in the Chang-Jaffé case where  $\nu_2$  is zero, and in the familiar Butler-Volmer case one must set  $\nu_2 = 1$ . The left-hand part of Fig. 1, when normalized to give  $Z_{CJN}$  involves  $C_{gN} \equiv C_g/C_g = 1$ ,  $R_{\infty N} \equiv 1$ , and  $Z_{SN}$ , where [4]

$$Y_{SN} \equiv Z_{SN}^{-1} = \rho_2 + i\Omega\psi^{-1}(\gamma_2 - 1) \quad (1)$$

where  $\psi \equiv 1 + i\Omega$ , and  $\gamma_2 \equiv (M_n\psi^{1/2})\text{ctnh}(M_n\psi^{1/2})$ . An important derived quantity is  $\gamma_{20} \equiv C_{DN} = (M_n)\text{ctnh}(M_n)$ , the  $\Omega \rightarrow 0$  limit of  $\gamma_2$ .

We shall now make an approximation which might seem to restrict the use of subsequent results to the low frequency region,  $\Omega \ll 1$ , but which turns out to be far less limiting. Expand  $\psi^{1/2} \equiv (1 + i\Omega)^{1/2}$  and  $\gamma_2$  to first order in  $\Omega$  to yield  $\psi^{1/2} \cong 1 + (i\Omega/2)$  and  $\gamma_2 \cong C_{DN} + i\Omega\epsilon_M$ , and neglect explicit  $\Omega^2$  terms in the numerator of eqn. (1). Here  $\epsilon_M \equiv 0.5[C_{DN} - (M_n^2)\text{csch}^2(M_n)]$  and approaches zero as  $M_n \rightarrow 0$ . Let us denote results obtained in this approximation by a prime. Then

$$Y'_{SN} = \rho_2 + i\Omega(C_{DN} - 1)/(1 + i\Omega) \quad (2)$$

This expression can be represented by a reaction resistance  $R_{RN} \equiv \rho_2^{-1}$  in parallel with the series combination of a resistance  $R_{SN} \equiv (C_{DN} - 1)^{-1}$  and a reaction capacitance  $C_{RN} \equiv (C_{DN} - 1)$ , where  $C_{DN}$  is the appropriate diffuse double layer capacitance. In the following we shall delete  $R_{SN}$  since it has little effect on the value of  $Y'_{SN}$  for  $\Omega \leq 0.1$  while at higher frequencies the contribution of  $Y_{SN}$  to  $Z_{CJN}$ , is usually overwhelmed by that of the other circuit elements. We thus obtain the approximate circuit (OAC) shown on the left side of Fig. 2a which agrees with the exact result previously obtained [4] in the  $\Omega \rightarrow 0$  limit.

The exact solution [2] for the  $Y_{SCN} \equiv Z_{SCN}^{-1}$  of Fig. 1 may be written as

$$Y_{SCN} = \frac{\rho_2[C_{CN}\{\rho_2\psi + i\Omega(\nu_2\rho_2 + \gamma_2[1 + \nu_2])\} + \nu_2\gamma_2(\rho_2\psi + i\Omega\gamma_2)]}{(\rho_2 + \gamma_2)[\rho_2(1 + i\Omega - \nu_2) + i\Omega\gamma_2]} \quad (3)$$

It should be noted that  $Y_{SCN}$  involves the quantity  $\gamma_2$  which is associated with processes in the bulk and diffuse layer. Since the potential drop across the

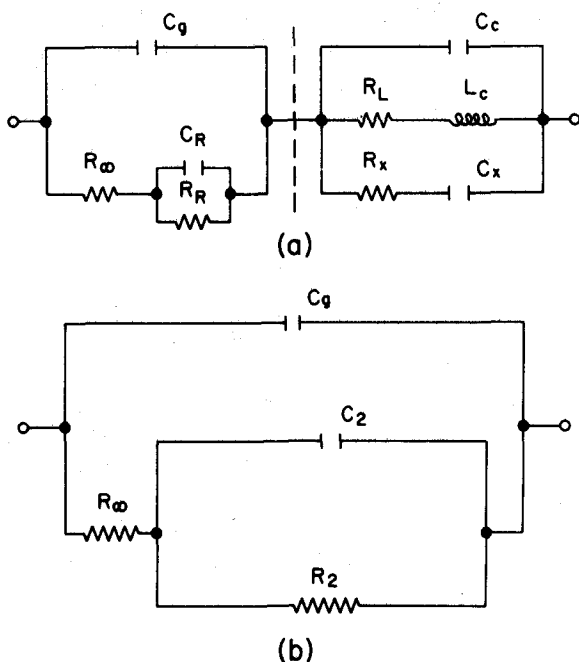


Fig. 2. Approximate equivalent circuits involving only frequency-independent elements. (a) Circuit for the first approximation. (b) Circuit for the second approximation when  $C_2 = \bar{C}_R$  and  $R_2 = \bar{R}_R$ .

compact layer is determined in part by processes in the diffuse layer and bulk, it is not possible to represent the effect of the compact layer by an equivalent circuit whose components are independent of the diffuse layer and bulk parameters. The total compact layer admittance (actually that for two identical electrodes) is then

$$Y_{CLN} \equiv Y_{SCN} + i\Omega C_{CN} \quad (4)$$

In the completely blocking situation, where  $\rho_2 = 0$ ,  $Y_{CLN} = i\Omega C_{CN}$ , and the compact layer contributes only the capacitance  $C_{CN}$ , which is in series with the left-hand circuit of Fig. 1. Let us again use the approximate form for  $\gamma_2$  and neglect  $\Omega^2$  terms separately in the numerator and denominator of eqn. (3). The result may be put in the following forms:

$$Y'_{SCN} = \frac{A + i\Omega B}{C + i\Omega D} = \frac{1}{(C/A) + i\Omega(D/A)} + \frac{i\Omega(B/C)}{1 + i\Omega(D/C)} \\ \equiv [R_{LN} + i\Omega L_{CN}]^{-1} + i\Omega C_{XN} [1 + i\Omega R_{XN} C_{XN}]^{-1} \quad (5)$$

The frequency-independent circuit elements appearing in the above are given by the following expressions:

$$R_{LN} \equiv (1 - \nu_2)(C_{DN} + \rho_2)[\rho_2(C_{CN} + \nu_2 C_{DN})]^{-1} \quad (6)$$

$$L_{CN} \equiv [(C_{DN} + \rho_2)^2 + \epsilon_M(1 - \nu_2)\rho_2][\rho_2^2(C_{CN} + \nu_2 C_{DN})]^{-1} \quad (7)$$

$$R_{\text{XN}} \equiv \frac{[(C_{\text{DN}} + \rho_2)^2 + \epsilon_{\text{M}}(1 - \nu_2)\rho_2]}{\rho_2[(C_{\text{DN}} + \rho_2)\{(1 + \nu_2)C_{\text{CN}} + \nu_2 C_{\text{DN}}\} + \epsilon_{\text{M}}\nu_2\rho_2]} \quad (8)$$

and

$$C_{\text{XN}} \equiv \frac{[(C_{\text{DN}} + \rho_2)\{(1 + \nu_2)C_{\text{CN}} + \nu_2 C_{\text{DN}}\} + \epsilon_{\text{M}}\nu_2\rho_2]}{(1 - \nu_2)(C_{\text{DN}} + \rho_2)} \quad (9)$$

The quantity  $R_{\text{LN}}$  had been previously denoted  $R_{\text{SCNO}}$ , the  $\Omega \rightarrow 0$  value of  $Z_{\text{SCN}}$ . These results lead directly to the circuit on the right side of Fig. 2a. Alternatively,  $Z'_{\text{SCN}}$  can be represented by an equivalent circuit made up of a resistance and capacitance in parallel ( $R_{\text{LN}}$  and  $C_{\text{XN}}$ ), in series with a resistance and inductance in parallel ( $R_{\text{XN}}$  and  $L_{\text{CN}}$ ). The choice is arbitrary since the impedance is the same for both representations at all frequencies. They both reduce to just  $R_{\text{XN}}$  and  $L_{\text{CN}}$  in parallel when  $\nu_2 = 1$ . We shall use the Fig. 2a representation but most attention will be given to the four circuit elements of  $Z'_{\text{SCN}}$  which are the same for either arrangement. Let the impedance of the entire circuit, which includes  $Z'_{\text{SN}}$  and  $Z'_{\text{SCN}}$ , be denoted by  $Z'_{\text{TN}}$ , while that where no approximations are made is denoted  $Z_{\text{TN}}$ .

### (III) DISCUSSION OF RESULTS

#### (a) Samples of macroscopic dimensions

In the Fig. 2a representation, the compact layer contribution to  $Z_{\text{TN}}$ ,  $Z'_{\text{CLN}} \equiv [Y'_{\text{SCN}} + i\Omega C_{\text{CN}}]^{-1}$ , involves an inductance in a resonant circuit. The inductive element does not, of course, imply the possibility of energy storage in a magnetic field, which is excluded in the model treated in our work, but simply expresses a phase relationship between processes in the compact and diffuse layers. The undamped resonant frequency  $\Omega_0 \equiv (L_{\text{CN}}C_{\text{CN}})^{-1/2}$  reduces to the simple form

$$\Omega_0 = \{[1 + (C_{\text{DN}}/C_{\text{CN}})]/[1 + (C_{\text{DN}}/\rho_2)^2]\}^{1/2} \quad (10)$$

when  $\nu_2 = 1$  (Butler-Volmer kinetics). In this case the damped and undamped resonant frequencies are the same.

The resonant character of  $Z'_{\text{CLN}}$  is a reflection of the exact behavior of  $Z_{\text{CLN}}$  and is not an artifact of the approximations made in Section II. This can be seen if one examines the percentage differences (p.d.'s) between the real of or imaginary parts of  $Z$  and  $Z'$ , i.e.  $100[\text{Re}(Z) - \text{Re}(Z')]/|Z|$  and  $100[\text{Im}(Z) - \text{Im}(Z')]/|Z|$ . For most conditions of interest, one finds that the maximum difference between the parts of  $Z_{\text{CLN}}$  and  $Z'_{\text{CLN}}$  is usually less than 1%, even at  $\Omega = 1$ , and rapidly approaches zero as  $\Omega \rightarrow 0$ . It should be noted however, that since the decomposition  $Z_{\text{TN}} \equiv Z_{\text{CJN}} + Z_{\text{CLN}}$  adopted here is not the only one possible, alternative equivalent circuits may be found with qualitatively different features.

We have already noted that  $Y_{\text{SN}}$  usually has only a small effect on  $Z_{\text{CJN}}$  when  $\Omega \geq 0.1$ , and thus the substitution of  $Y'_{\text{SN}}$  for  $Y_{\text{SN}}$  introduces only small errors in  $Z_{\text{CJN}}$ . Therefore,  $Z'_{\text{TN}} \equiv Z'_{\text{CJN}} + Z'_{\text{CLN}}$  will usually well approximate  $Z_{\text{TN}} \equiv Z_{\text{CJN}} + Z_{\text{CLN}}$  even for  $\Omega \sim 1$ . For parameter values  $M = 10^4$ ,  $C_{\text{CN}} = 10^3$ ,

$\rho_2 = 1$  and  $\nu_2 = 0.5$ , for example, one finds the maximum p.d.'s between the real and imaginary parts of  $Z'_{\text{TN}}$  and  $Z_{\text{TN}}$  to occur in the region  $\Omega = 0.01$  to  $0.1$  and be less than  $0.01\%$ ! Further explicit results will be presented below. Similar excellent agreement is found for other sets of system parameters when  $M$  and  $C_{\text{CN}} \gg 1$ . Thus conclusions drawn from the circuit of Fig. 2a follow as well from the exact results for all  $\Omega$  when  $M$  and  $C_{\text{CN}}$  are large. Slightly modified conclusions must be drawn for the region  $\Omega \geq 0.1$  in the thin film or membrane case, where  $C_{\text{CN}} \sim 1$ . Thin film and membrane response will be discussed in some detail later in this work.

In the completely blocking situation ( $\rho_2 = 0$ ),  $R_{\text{RN}} = L_{\text{CN}} = R_{\text{XN}} = \infty$  and  $Z'_{\text{CLN}}$  reduces simply to  $C_{\text{CN}}$  in series with the left-hand circuit. As  $\Omega$  approaches zero, the total parallel capacitance of the system,  $C_{\text{PN}}$ , appearing in  $Y'_{\text{TN}}$  or  $Y_{\text{TN}} \equiv Z_{\text{TN}}^{-1} \equiv G_{\text{PN}} + i\Omega C_{\text{PN}}$ , approaches its  $\Omega = 0$  value,  $C_{\text{PNO}} = [C_{\text{DN}}^{-1} + C_{\text{CN}}^{-1}]^{-1}$ , the conventional result, thus exactly justifying in this completely blocking case, but only in this case, the conventional separation of double-layer differential capacitance results into compact layer and diffuse layer contributions.

Another limiting case is that in which  $\nu_2 = 1$ , as for Butler-Volmer kinetics. Then  $R_{\text{LN}} \rightarrow 0$  and  $C_{\text{XN}} \rightarrow \infty$ , leaving just  $C_{\text{CN}}$ ,  $L_{\text{CN}}$  and  $R_{\text{XN}}$  in parallel. This is not a situation where  $R_{\text{XN}}$  is always so small that it dominates the impedance. The quality factor at  $\Omega = \Omega_0$ ,  $Q_0 \equiv R_{\text{XN}}[C_{\text{CN}}/L_{\text{CN}}]^{1/2}$ , can readily be of the order of unity. Consider, for example, the situation where  $C_{\text{DN}} \gg \rho_2$ . Then

$$Q_0 \simeq \left[ \frac{C_{\text{CN}}(C_{\text{CN}} + C_{\text{DN}})}{(2C_{\text{CN}} + C_{\text{DN}})^2} \right]^{1/2} \quad (11)$$

a quantity which approaches its maximum value of  $0.5$  when  $C_{\text{CN}} \gg C_{\text{DN}}$ . Even when  $C_{\text{DN}} = 10^4/\sqrt{2}$ ,  $C_{\text{CN}} = 10^3$ , and  $\rho_2 = 0.1$ ,  $Q_0 \simeq 0.31$ . On the other hand, for  $\rho_2 \gg C_{\text{DN}}$  one finds that  $Q_0$  approaches  $(1 + \nu_2)^{-1}$  when  $C_{\text{CN}} \gg C_{\text{DN}}$  as well. The compact layer impedance,  $Z'_{\text{CLN}}$ , is by no means negligible compared to  $Z'_{\text{CJN}}$ . For example, for  $M = C_{\text{CN}} = 10^4$ ,  $\rho_2 = 0.1$ , and  $\nu_2 = 1$ ,  $Z'_{\text{CLN}}$  and  $Z'_{\text{CJN}}$  are respectively,  $1.869 + 1.179i$  and  $7.667 - 4.714i$  for  $\Omega = 10^{-5}$ , and  $0.3547 - 0.8948i$  and  $1.196 - 1.387i$  for  $\Omega = 10^{-4}$ . These values are negligibly different from  $Z_{\text{CLN}}$  and  $Z_{\text{CJN}}$  here. Note that the resonant frequency must lie between these values of  $\Omega$  since  $\text{Im}(Z'_{\text{CLN}})$  changes sign between them. It is actually found to occur at  $\Omega \cong 1.848 \times 10^{-5}$ . The normalization of the pseudo-inductance  $L_{\text{C}}$  used here is  $L_{\text{CN}} \equiv L_{\text{C}}/\tau_{\text{D}}R_{\infty}$ . In the present case,  $L_{\text{CN}} \cong 2.93 \times 10^5$ . For the typical values  $C_{\text{g}} = 10$  pF and  $R_{\infty} \equiv 10^3 \Omega$ , one finds that the above value of  $L_{\text{CN}}$  corresponds to  $L_{\text{C}} \cong 2.93$  H, a substantial inductance were it real.

The fast reaction case,  $\rho_2 \rightarrow \infty$ , is also of interest. For  $\nu_2 = 1$ ,  $Y_{\text{SCN}}$  involves a term proportional to  $(i\Omega)^{-1}$  and thus becomes infinite at  $\Omega = 0$ . The compact layer thus contributes nothing at  $\Omega = 0$ . Although  $|Y_{\text{SCN}}|$  is not infinite for  $\Omega > 0$  in this case, it will be very large for the present  $C_{\text{CN}}$  and/or  $C_{\text{DN}} \gg 1$  case. Then  $|Z_{\text{CJN}}| \gg |Z_{\text{CLN}}|$  and only bulk behavior will appear. When  $\nu_2 \neq 1$ ,  $R_{\text{LN}}$ ,  $L_{\text{CN}}$ ,  $R_{\text{XN}}$ , and  $C_{\text{XN}}$  are all non-zero but the time constants  $R_{\text{XN}}C_{\text{XN}}$  and  $L_{\text{CN}}/R_{\text{LN}}$  both become  $(1 - \nu_2)^{-1}$ . Further  $\Omega_0 \rightarrow [1 + (\nu_2 C_{\text{DN}}/C_{\text{CN}})]^{1/2}$ , always greater than unity when  $\nu_2 > 0$ . ( $\nu_2 < 0$  is improbable since it implies a decrease in overall reaction rate with increasing overpotential.) The very fast reaction situation will be further discussed at the end of this Section.

In the general  $\nu_2 \neq 1$  case with  $\rho_2 \ll C_{\text{DN}}$ , one again finds that the contribu-

tion of  $Z'_{CLN}$  to  $Z'_{TN} \equiv Z'_{CJN} + Z'_{CLN}$  is often very significant. For example, for  $M = 10^4$ ,  $C_{CN} = 10^3$ ,  $\rho_2 = 1$ , and  $\nu_2 = 0.5$ , one obtains  $C_{DN} \cong 7.071 \times 10^3$ ,  $C_{RN} \cong 7.070 \times 10^3$ ,  $R_{RN} = 1$ ,  $R_{LN} \cong 0.7796$ ,  $L_{CN} \cong 1.103 \times 10^4$ ,  $R_{XN} = 1.404$ , and  $C_{XN} \cong 1.007 \times 10^4$ . The resonant circuit is here more complicated and loaded resonance no longer occurs exactly at  $\Omega = \Omega_0$ . At  $\Omega = 10^{-4}$ ,  $Z'_{CLN}$  and  $Z'_{CJN}$  are, respectively,  $1.071 + 0.2006i$  and  $1.667 - 0.4716i$ . Differences between primed and unprimed quantities occur here only in the fifth or sixth decimal place and have only reached the third decimal place by  $\Omega = 0.1$ .

Although  $Z_{CLN}$  shows strong resonant behavior and makes by no means a negligible contribution to  $Z_{CJN}$  in the  $\Omega$  region where  $|\text{Im}(Z_{TN})|$  is a maximum, the total impedance,  $Z_{TN}$  or  $Z'_{TN}$ , often turns out to be much simpler than one might expect from the above, and an exceptionally simple equivalent circuit can be found which reproduces  $Z'_{TN}$  (and even  $Z_{TN}$ ) over the usual  $\Omega$  range of interest to high accuracy when  $M$  and  $C_{CN} \gg 1 + \rho_2$ .

Remember that all the circuit elements of Fig. 1 or Fig. 2a when reduced to normalized form depend only on the four parameters  $\rho_2$ ,  $\nu_2$ ,  $M$ , and  $C_{CN}$ . Therefore, as shown by eqns. (6)–(9), the elements of  $Z_{CLN}$  must be interdependent. This suggests, along with numerical results for  $Z_{TN}$ , that we search for a simpler equivalent circuit with only four circuit elements. One of the simplest, consistent with explicit recognition of bulk response when  $M$  and  $C_{CN}$  are large, is shown in Fig. 2b, just the ordinary equivalent circuit found without compact layer effects but with its reaction-related circuit elements modified.

To find the simplest and most appropriate values of the frequency-independent elements  $C_{2N}$  and  $R_{2N}$  of Fig. 2b, let us require that the impedance of the Fig. 2b circuit,  $\bar{Z}_{TN}$ , agrees exactly with that of Fig. 2a,  $Z'_{TN}$ , and with  $Z_{TN}$  as  $\Omega \rightarrow 0$ . A bar will be used to identify impedances and circuit elements following from the circuit of Fig. 2b when this limiting condition is imposed. One finds

$$R_{2N} = \bar{R}_{RN} \equiv R_{RN} + R_{LN} = \rho_2^{-1} \left[ \frac{C_{CN} + C_{DN} + \rho_2(1 - \nu_2)}{C_{CN} + \nu_2 C_{DN}} \right] \quad (12)$$

and

$$C_{2N} = \bar{C}_{RN} \equiv \frac{R_{RN}^2 C_{RN} + R_{LN}^2 (C_{CN} + C_{XN} - 1) - [L_{CN} + 2(1 + R_{RN})R_{LN}]}{(R_{RN} + R_{LN})^2} \quad (13)$$

When  $\nu_2 = 1$ ,  $\bar{R}_{RN}$  reduces to just  $R_{RN} = \rho_2^{-1}$  and  $\bar{C}_{RN}$  becomes

$$\bar{C}_{RN} = C_{RN} - \frac{(C_{DN} + \rho_2)^2}{C_{DN} + C_{CN}} = \frac{C_{DN}[C_{CN} - (1 + 2\rho_2)] - (C_{CN} + \rho_2^2)}{(C_{DN} + C_{CN})} \quad (14)$$

Equation (14) indicates that when  $C_{RN}$  and  $C_{CN}$  are both much larger than  $(1 + \rho_2)$ , the usual non-membrane case of interest,  $\bar{C}_{RN} \cong (C_{RN}^{-1} + C_{CN}^{-1})^{-1} \equiv C_{SN} \cong (C_{DN}^{-1} + C_{CN}^{-1})^{-1}$ . When  $\rho_2 = 0$ , the exact result  $C_{PNO} = 1 + \bar{C}_{RN} = [C_{DN}^{-1} + C_{CN}^{-1}]^{-1}$  is again found. Thus, to the degree that  $\bar{Z}_{TN}$  is a good approximation to  $Z_{TN}$  over the range of  $\Omega$  of interest, the entire effect of the compact layer, when  $M$  and  $C_{CN}$  are  $\gg 1 + \rho_2$ , is to change  $R_R$  to  $(R_R + R_L)$  and to add  $C_C$  in series with  $C_R$ ! The degree to which  $\bar{C}_{RN}$  actually approximates  $C_{SN}$  is shown for a few varied situations in Table 1.

Let us still restrict attention to samples of macroscopic thickness so  $M$  and

TABLE I  
Input parameters and resulting normalized circuit element values for various cases

	$\rho_2$	$\nu_2$	$C_{CN}$	$M$	$L_{CN}$	$R_{XN}$	$\bar{R}_{RN}$	$\bar{C}_{RN}$	$C_{SN}$
A	1	1	$10^3$	$10^6$	$7.061 \times 10^5$	0.9972	1	995.59	998.59
B	0.1	1	$10^4$	$10^4$	$2.929 \times 10^5$	2.612	10	$4.1411 \times 10^3$	$4.1418 \times 10^3$
C	0.1	1	$10^3$	$10^4$	$6.195 \times 10^5$	7.795	10	874.93	876.09
D	$\infty$	1	$10^3$	$10^4$	$1.239 \times 10^{-4}$	$7.932 \times 10^{-5}$	0	$-\infty$	876.09
E	1	0.5	$10^3$	$10^4$	$1.103 \times 10^4$	1.404	1.7796	874.09	876.09
F	0.1	0	$10^3$	$10^4$	$5.000 \times 10^6$	70.71	80.71	875.07	876.09

$C_{CN} \gg 1$ . For example, if  $l = 0.4$  cm,  $L_D = 2 \times 10^{-5}$  cm, and  $d$ , the thickness of the compact layer, were  $2 \times 10^{-8}$  cm, then  $M = 10^4$  and  $C_{CN} \approx 10^7$ , provided the dielectric constants of the compact layer region and the bulk of the sample are approximately equal. Usually, that for the compact layer region will be smaller than that of the main material of interest. Since  $C_{DN}$  is  $10^4/\sqrt{2}$  here, and  $C_{CN}/C_{DN} \gg 1$ , one finds  $\bar{C}_{RN} \approx C_{SN} \approx C_{DN}$ , leading to no appreciable compact layer effect in  $\bar{C}_{RN}$ . If  $\nu_2 = 1$  as well,  $\bar{R}_{RN} = R_{RN} = \rho_2^{-1}$ , with no compact layer effect at all. For  $\nu_2 = 0.5$  and  $\rho_2 = 1$ , one calculates  $R_{RN} = 1$ ,  $R_{LN} \approx 3.53 \times 10^{-4}$ , and thus  $\bar{R}_{RN} \approx 1.0004$ , again an entirely negligible effect. In situations such as this, the entire effect of the compact layer is negligible. But under high concentration conditions, for appreciable intrinsic space-charge (Frenkel) layers or d.c. biasing potentials, which increase  $C_{DN}$  greatly, and for superionic conductors, one may find even for samples of macroscopic thickness that  $C_{CN}/C_{DN} \lesssim 1$  and even that  $C_{CN} \ll C_{DN}$ . When  $M$  and  $C_{CN} \gg (1 + \rho_2)$  and  $C_{CN}/C_{DN} \ll 1$ , we have seen that  $\bar{C}_{RN} \approx C_{SN}$ , which in this case approaches just  $C_{CN}$ . When these conditions remain satisfied, we thus expect that  $\bar{C}_{RN}$  will be virtually independent of temperature and applied potential near zero current, as found by Armstrong et al. [5,6] for  $\beta$ -alumina, and  $\bar{C}_{RN}$  will be independent of concentration as well.

Let us compare exact and approximate results for a few macroscopic situations where the compact layer leads to measurable effects. Note that when the time constants of the Fig. 2b circuit are well separated, so  $R_{\infty}C_g \ll \bar{R}_R\bar{C}_R$ , a plot of  $\bar{Z}_{TN}^*$  in the complex plane as a parametric function of  $\Omega$  leads to two adjoining semicircles with a sharp cusp between them [1,4,7,8], the bulk one extending on the real axis from  $\text{Re}(\bar{Z}_{TN}^*) = 0$  to 1 and the reaction one from 1 to  $1 + \bar{R}_{RN}$ , the normalized zero-frequency resistance,  $R_{DN}$ . Thus unless  $\bar{R}_{RN}$  is greater than perhaps 0.01, the combined compact layer/reaction processes will be of negligible importance.

Table 1 summarizes some typical input parameter situations and the resulting normalized circuit element values. For simplicity, we have not listed  $R_{RN} = \rho_2^{-1}$ ,  $C_{RN}$  [which is here well approximated by  $(2^{-1/2}M - 1)$ ],  $R_{LN}$ , and  $C_{XN}$ . In cases E and F,  $R_{LN} \approx 0.7796$  and 70.71, respectively, and is zero for the other cases. Similarly,  $C_{XN} = 1.0072 \times 10^4$  and  $10^3$  for E and F, and is otherwise infinite. In the infinite-reaction-rate situation of case D, no compact layer/reaction effects occur and only bulk effects remain.

Table 2 shows some impedance results for several of the cases of Table 1 at three normalized frequencies. The agreement between the exact  $Z_{TN}$  results and the  $Z'_{TN}$  and  $\bar{Z}_{TN}$  approximations must be exact as  $\Omega \rightarrow 0$ ; it is still remarkably good at  $\Omega = 10^{-4}$ , with  $Z'_{TN}$  being slightly closer than  $\bar{Z}_{TN}$  to  $Z_{TN}$ . The similarity in most of the results for  $\Omega = 10^{-2}$  and for all at  $\Omega = 0.1$  arises because bulk effects begin to dominate the impedance in this frequency region, and, with bulk parameter normalization, bulk impedance is independent of specific input parameters. Results are shown for  $10^{-2}$  and 0.1, however, because percentage differences, as defined earlier, between the parts of the various impedances are generally largest in this range. Again we see that  $Z'_{TN}$  is remarkably close to  $Z_{TN}$  even in this region and that even  $\bar{Z}_{TN}$  is an excellent approximation. Since the circuit of Fig. 2b is much simpler than that of 2a, it is therefore clear that 2b and  $\bar{Z}_{TN}$  may be used in place of either  $Z_{TN}$  or  $Z'_{TN}$  for any  $\Omega$  in all cases of

TABLE 2

Exact and approximate normalized impedance results for some Table 1 cases

		$\Omega = 10^{-4}$	$\Omega = 10^{-2}$	$\Omega = 0.1$
A	$Z_{TN}$	1.99013 - 0.098973i	1.00983 - 0.109146i	0.990197 - 0.109023i
	$Z'_{TN}$	1.99013 - 0.098973i	1.00983 - 0.109146i	0.990197 - 0.109023i
	$\bar{Z}_{TN}$	1.99015 - 0.098977i	1.00788 - 0.109510i	0.988231 - 0.108767i
B	$Z_{TN}$	1.55054 - 2.28139i	0.999746 - 0.0341387i	0.989891 - 0.101398i
	$Z'_{TN}$	1.55046 - 2.28139i	0.999676 - 0.0341372i	0.989822 - 0.101382i
	$\bar{Z}_{TN}$	1.55031 - 2.28150i	0.999476 - 0.0341354i	0.989626 - 0.101353i
C	$Z_{TN}$	6.65741 - 4.95679i	1.00099 - 0.124125i	0.989903 - 0.110398i
	$Z'_{TN}$	6.65726 - 4.95677i	1.00092 - 0.124122i	0.989835 - 0.110382i
	$\bar{Z}_{TN}$	6.65753 - 4.95768i	0.998922 - 0.124141i	0.987875 - 0.110092i
F	$Z_{TN}$	2.58235 - 11.19060i	0.999849 - 0.124139i	0.989892 - 0.110398i
	$Z'_{TN}$	2.58226 - 11.19055i	0.999779 - 0.124137i	0.989823 - 0.110382i
	$\bar{Z}_{TN}$	2.58040 - 11.19116i	0.997780 - 0.124113i	0.987864 - 0.110088i

interest when  $M$  and  $C_{CN} \gg (1 + \rho_2)$ . Incidentally, even at  $\Omega = 10^{-2}$  in cases A, C, E, and F,  $|\text{Im}(Z_{CLN})| > |\text{Im}(Z_{CJN})|$ , showing that the compact layer still makes an important contribution to the total impedance even at this frequency.

When impedance measurements on an appropriate system are compared [8] with the predictions of Fig. 2b, estimates of  $R_\infty$ ,  $C_g$ ,  $\bar{R}_R$ , and  $\bar{C}_R$  may be obtained. Then  $\bar{R}_{RN}$  and  $\bar{C}_{RN}$  estimates may be formed. These two quantities, which very adequately determine  $Z_{TN}$ , are insufficient to allow estimation of the four parameters  $\rho_2$ ,  $\nu_2$ ,  $C_{CN}$  and  $C_{DN}$ . Fortunately,  $\nu_2$  may be determined separately by steady-state direct current-voltage measurements near zero current, and  $C_{CN}$  may often be estimated from knowledge of the size of the charge carrier, crystal structure, or from differential capacitance measurements. In the present case, where  $M$  and  $C_{CN} \gg (1 + \rho_2)$ , one can obtain  $C_{RN}$  and thus  $C_{DN}$  from  $\bar{C}_{RN}$  if  $C_{CN}$  is known or  $C_{CN}$  from  $\bar{C}_{RN}$  if  $C_{DN}$  is known. The characterization process will be aided if measurements at several different values of mobile charge concentrations can be carried out in order to vary the values of  $M$  and  $C_{DN}$  and thus facilitate the separation of  $C_{DN}$  and  $C_{CN}$ .

The calculation of the reaction rate constant,  $k_2$ , which requires the determination of  $\rho_2$ , is of particular interest when  $\nu_2 \neq 1$ . When  $\nu_2 = 1$ , we can obtain  $\rho_2$  directly from  $\bar{R}_{RN} = \rho_2^{-1}$ . But in general, eqn. (12) shows that

$$\rho_2^{-1} = (C_{CN} + C_{DN})^{-1} [(C_{CN} + \nu_2 C_{DN}) \bar{R}_{RN} - (1 - \nu_2)] \quad (15)$$

Thus, when  $\nu_2 \neq 1$  it is clearly incorrect to neglect the compact layer effect on the effective reaction rate and assume that  $\rho_2^{-1} = \bar{R}_{RN}$ . The relative compact layer correction to  $\bar{R}_{RN}$ ,  $R_{LN}/R_{RN}$  equals  $(\nu_2^{-1} - 1)$  and is independent of  $\rho_2$  when  $C_{DN} \gg C_{CN}$ . But when  $C_{DN} \ll C_{CN}$  it approaches  $(1 - \nu_2)\rho_2/C_{CN}$  and can clearly be large when  $\rho_2 \gg C_{CN}$ . This need not imply a fast reaction rate ( $\rho_2 \gg 1$ ) if  $C_{CN}$  is small, as in a membrane situation. Consider the intermediate case in which  $C_{CN} = C_{DN} = \rho_2 = 10^3$  and  $\nu_2 = 0.5$ . Then,  $(R_{LN}/R_{RN}) = 2/3$ ,  $(C_{CN} + \nu_2 C_{DN}) \bar{R}_{RN} = 2.5$ , and  $(1 - \nu_2) = 0.5$ . Thus, the  $(1 - \nu_2)$  term in eqn. (15) cannot be neglected here.

Consider next the fast reaction limit,  $\rho_2 \rightarrow \infty$ . When  $\nu_2 = 1$ ,  $\bar{C}_{RN} \rightarrow -\infty$  and  $\bar{R}_{RN} \rightarrow 0$ , implying no compact layer contributions to the total impedance. We have already seen, from consideration of the accurate  $Z_{SCN}$  expression, however, that this conclusion is true for  $\Omega = 0$  but only approximately true for  $\Omega > 0$ . When  $C_{CN}$  and  $C_{DN}$  are small (see next Section), the  $Z_{CLN}$  contribution to  $Z_{TN}$  will not be negligible (except near  $\Omega = 0$ ) for  $\rho_2$  very large and  $\nu_2 = 1$ .

The situation is somewhat different for  $\rho_2$  very large and  $\nu_2 \neq 1$ . Equation (12) leads to

$$\bar{R}_{RN} = R_{LN} \cong (1 - \nu_2)/(C_{CN} + \nu_2 C_{DN}) \quad (16)$$

a non zero result even for  $\rho_2$  arbitrarily large. This apparent reaction resistance, which may even be negative, is independent of  $\rho_2$  for  $\rho_2 \gg (1 - \nu_2)^{-1}(C_{CN} + C_{DN})$  and arises entirely from the presence of the compact layer and non-Butler-Volmer kinetics. It thus establishes a maximum actual reaction rate which can be determined from small-signal a.c. methods. While  $\bar{C}_{RN} = -\infty$  for  $\nu_2 = 1$ , when  $\nu_2 \neq 1$   $\bar{C}_{RN}$  is finite. It is negative for  $\nu_2 > 10$  if  $C_{DN} \gg C_{CN} \gg 1$ . Although the finite value of  $\bar{C}_{RN}$  will affect the response for  $\Omega > 0$ , it has no influence at  $\Omega = 0$  where one determines  $R_D$ ,  $R_{DN}$ , and  $\bar{R}_{RN}$ .

Let us define an effective boundary parameter  $\bar{\rho}_2^\infty$  by

$$\bar{\rho}_2^\infty = \bar{R}_{RN}^{-1} \Big|_{\rho_2 \rightarrow \infty} = (1 - \nu_2)^{-1}(C_{CN} + \nu_2 C_{DN}) \quad (17)$$

which is related to the apparent limiting reaction rate constant by [1,2]

$$\bar{k}_2^\infty = (l/2)^{-1} D_2 \bar{\rho}_2^\infty \quad (18)$$

where  $D_2$  is the diffusion coefficient for negative charge carriers. Note that since both  $C_{CN}$  and  $C_{DN}$  are proportional to  $l$  (for  $M \geq 5$ ),  $\bar{k}_2^\infty$  is intensive as it should be. To summarize, for non-Butler-Volmer kinetics the presence of the compact layer causes a finite electrode reaction resistance to appear, even if the electrode reaction is extremely fast. In this sense,  $Z_{CLN}$  or  $Z'_{CLN}$  should not be entirely neglected when  $\rho_2$  is very large. To see the possible order of magnitude of  $\bar{k}_2^\infty$ , take  $l = 0.1$  cm,  $D_2 = 10^{-5}$  cm<sup>2</sup> s<sup>-1</sup>,  $\nu_2 = 0.5$ ,  $C_{CN} = 10^7$ , and  $C_{DN} = 2 \times 10^4$ . Then eqn. (17) leads to  $\bar{\rho}_2^\infty \cong 2 \times 10^7$  and  $\bar{k}_2^\infty \cong 10$  s<sup>-1</sup>.

But notice that for the above input values,  $\bar{\rho}_2^\infty = 2 \times 10^7$  will not be experimentally determinable. As  $\Omega \rightarrow 0$  one actually measures  $R_{DN} = 1 + \bar{R}_{RN}$ , negligibly different from 1 (arising from  $R_\infty$  alone) in the present case. Suppose we find that we can only determine  $\bar{R}_{RN}$  from  $R_{DN}$  adequately when  $\bar{R}_{RN} \geq 0.01$ . Then  $\bar{\rho}_2^\infty \leq 100$  and, for the above values,  $\bar{k}_2^\infty \leq 5 \times 10^{-5}$  s<sup>-1</sup>, a slow reaction. Further, this condition leads to  $(C_{CN} + \nu_2 C_{DN}) \leq 100(1 - \nu_2)$ , satisfied only for very thin films or membranes when  $\nu_2 \neq 1$ . Thus the  $\bar{\rho}_2^\infty$  limitation on  $\rho_2$  determination will generally only be of importance in such situations. Incidentally, since  $R_\infty \propto l$  and  $\bar{R}_R$  is independent of  $l$ , measurements of the same material for several differing  $l$ 's will aid in the separation of  $R_\infty$  and  $\bar{R}_R$ .

The results obtained in this Section have led us to further consider our recent discussion [3] of the work of Kornyshev and Vorotyntsev [9] on the small-signal a.c. response of solid electrolytes. We there stated that the admittance expression obtained by those authors was valid only for  $\Omega \ll 1$  since it agreed with our exact result only in that frequency range. The considerations treated in this paper, however, indicate that the analytical result of Kornyshev

and Vorotyntsev, though approximate, should quite accurately describe the observable response at all frequencies for systems of macroscopic dimensions having  $\nu_2 = 1$  satisfying the other criteria stated in their work. It may also be noted that values of  $R_2$  and  $C_2$  may readily be found for which the equivalent circuit of Fig. 2b reproduces their impedance result to within the approximations made in their work, which did not explicitly deal with equivalent circuit representations.

(b) *Thin films and membranes*

Consider now films or membranes so thin that the compact layer thickness is appreciable compared to the total electrode separation,  $l$ . Then we may expect that  $C_{CN}$  will fall in the range 0.1 to  $10^2$ . Since  $l$  will be very small,  $M$  and  $C_{DN}$  will no longer usually fall in the range of  $10^3$  to  $10^6$  but may be as small as unity or less. Compact layers have been considered previously in the theory of ultrathin membranes, and de Levie and Abbey [10] have obtained a theoretical expression for the admittance of a membrane with compact layers. It should be noted, however, that the assumptions made by these authors differ in essence from those in our original work, their treatment being applicable to the case of charge injection into a membrane without compensating background charge, ours to the case of intrinsic charge within the membrane.

To investigate some of the possibilities let us temporarily consider only  $\nu_2 = 1$ . Then  $\bar{R}_{RN} = \rho_2^{-1}$ . Equation (14) leads to the following conclusions, which of course are only of interest under conditions where  $\bar{Z}_{TN} \cong Z_{TN}$ . First, when  $C_{CN} \gg C_{DN}$  and  $\rho_2$ ,  $\bar{C}_{RN} \cong C_{RN}$ , and no appreciable compact layer effects are present. When  $\rho_2 = 0$ ,  $\bar{C}_{RN} + 1 = C_{DN}^{-1} + C_{CN}^{-1}$ , independent of the size of  $C_{CN}$  and  $C_{DN}$ . Note that no matter how small  $M$ , the minimum value of  $C_{DN}$  is unity.

When  $C_{CN} = \rho_2$ ,  $C_{RN} = -(1 + \rho_2) = -(1 + C_{CN})$ , negative and entirely independent of  $M$  for any  $M$ !  $\bar{C}_{RN}$  is also independent of  $M$  when  $C_{DN} \gg C_{CN}$  and  $\rho_2^2$ , but this holds only over a limited range of  $M$ . In this case  $\bar{C}_{RN} \cong C_{CN} - 1 - 2\rho_2$ , which may also be negative. Finally,  $\bar{C}_{RN}$  may be zero. This occurs when  $C_{CN} = [\rho_2^2 + C_{DN}(1 + 2\rho_2)]/C_{RN}$ . For large  $M$ , this expression approaches  $(1 + 2\rho_2)$ . When  $\nu_2 \neq 1$ ,  $\bar{C}_{RN}$  may still be negative for many conditions.

Table 3 presents input and output values for various situations with  $C_{CN}$  relatively small. Here we have used  $M_n = M/\sqrt{2}$  as an input and explicitly shown  $C_{RN}$  values. For case H,  $R_{LN} = 0.6982$  and  $C_{XN} = 4.440$ ; for the other cases  $R_{LN} = 0$  and  $C_{XN} = \infty$ . The series capacitance  $C_{SN}$  is not shown explicitly here since it is usually far different from  $\bar{C}_{RN}$  in these small  $C_{CN}$  situations. For case K,  $C_{SN} = 9.083$ .

Because of the small value of  $C_{CN}$ , impedance plane plots for the cases of Table 3 no longer show separate bulk and compact layer/reaction semicircles with a sharp cusp between them. Instead there is melding of various kinds. The  $\Omega \rightarrow 0$  normalized resistance,  $R_{DN}$ , is 11 in cases A–E and I–K. It is  $10^3$  for F, 2 for G, and 2.7 for H. For cases A–C, the normalized impedance plot yields an arc with nearly a straight-line portion at an angle of about  $45^\circ$  smoothly melding into the arc of a circle with radius about 5. The maximum value of  $|\text{Im}(Z_{TN})|$  is about 5 and occurs near  $\Omega = 0.1$ , a value arising from  $C_{eN}\bar{R}_{RN}\Omega = \bar{R}_{RN}\Omega = 1$ . These curves could possibly erroneously be identified

TABLE 3  
Input parameters and resulting normalized circuit element values for various cases

	$\rho_2$	$\nu_2$	$C_{CN}$	$M_n$	$C_{RN}$	$L_{CN}$	$R_{XN}$	$\bar{R}_{RN}$	$\bar{C}_{RN}$
A	0.1	1	1	$10^4$	9999	$9.999 \times 10^5$	9.998	10	-0.2001
B	0.1	1	1	10	9	$9.274 \times 10^2$	8.382	10	-0.2736
C	0.1	1	1	3	2.015	$2.417 \times 10^2$	6.154	10	-0.4017
D	0.1	1	1	1	0.3130	$8.632 \times 10^1$	4.238	10	-0.5502
E	0.1	1	1	$10^{-4}$	$3.33 \times 10^{-9}$	$6.050 \times 10^1$	3.666	10	-0.6050
F	$10^{-3}$	1	1	$10^{-4}$	$3.33 \times 10^{-9}$	$5.010 \times 10^5$	$3.336 \times 10^2$	$10^3$	-0.5010
G	1	1	1	1	0.3130	2.313	0.6723	1	-2
H	1	0.5	1	1	0.3130	3.319	1.070	1.698	-1.260
I	0.1	1	10	0.1	$3.331 \times 10^{-3}$	$1.106 \times 10^1$	0.5253	10	-0.1073
J	0.1	1	10	1	0.3130	$1.765 \times 10^1$	0.6623	10	-0.1365
K	0.1	1	10	$10^2$	99	$9.109 \times 10^3$	8.338	10	7.909

as of finite Warburg form [4,7] judging by shape alone. No separate bulk semicircle is at all apparent here.

The plots for cases D–I are also very instructive. They are nearly perfect semicircles with radius  $R_{DN}/2$ . If compact layer effects of the present type were present but ignored, one would surely identify such semicircles with pure bulk behavior. But this would be wrong. Even when  $\nu_2 = 1$  and  $R_{LN} = 0$ ,  $R_{DN}$  may differ greatly from  $R_{\infty N} \equiv 1$ . In case D, for example,  $R_{DN} = 11$ .

It is of interest to examine the constancy of the radius of the case D arc assuming that it approximates a semicircle with center at  $\text{Re}(Z_{TN}) = R_{DN}/2 = 5.5$  and  $\text{Im}(Z_{TN}) = 0$ . We therefore compare  $[\{\text{Re}(Z_{TN}) - 0.5R_{DN}\}^2 + \{\text{Im}(Z_{TN})\}^2]^{1/2}$  with 5.5. The following values are obtained:  $\Omega = 10^{-2}$ , 5.4998;  $\Omega = 10^{-1}$ , 5.488;  $\Omega = 1$ , 5.459; and  $\Omega = 10$ , 5.495. The arc is nearly, but not exactly, semicircular.

To investigate the degree to which nearly semicircular arcs, such as those obtained in cases D–I, can be well represented by simple equivalent circuits involving frequency-independent elements, we have fitted 37 exact  $Z_{TN}(\Omega)$  values calculated for case D for the range  $10^{-8} \leq \Omega \leq 10$  by unweighted complex least squares [8]. The  $\Omega$  values were uniformly distributed in  $\log \Omega$ . Fitting to the impedance of a single resistance  $R_N$  in parallel with a single capacitance  $C_N$  yielded a good fit with  $R_N \cong 10.9986 \pm 0.0021$  and  $C_N \cong 0.5447 \pm 0.0006$ , where the standard deviations listed here are only indicative since they arise entirely from systematic rather than random disagreement between “data” and model. The value of  $R_N$  found is satisfyingly close to  $R_{DN} = 11$ . The  $C_N$  value is a complicated mixture of  $C_{\infty N} \equiv 1$  and  $\bar{C}_{RN} = -0.5502$ . As expected, the fit between model and data was better at small  $\Omega$  values than at large ones. In addition, a fit was carried out to a circuit of the form of that of Fig. 2b with the quantities  $R_{\infty N}$  and  $C_{\infty N}$  replaced by  $R_{1N}$  and  $C_{1N}$ . This fit reduced completely to the first one, showing that a better fit could not be obtained in this case with four instead of two free frequency-independent circuit elements.

As  $M_n$  increases from the value of 1 in case J to 100 in case K, the good semicircle found in case J begins to distort and by  $M_n = 10$  a considerable portion of the bulk semicircle, radius 0.5, appears before it melds smoothly into the compact layer/reaction semicircle, radius 5. By  $M_n = 100$  of case J, even more of the bulk semicircle is apparent at the high  $\Omega$  end of the data. There is, however, no maximum present in  $|\text{Im}(Z_{TN})|$  in passing from the bulk part of the curve to the beginning of the low frequency semicircle.

Finally, one may ask how good the  $Z'_{TN}$  and  $\bar{Z}_{TN}$  approximations turn out to be in the present cases. A few representative impedance results are listed in Table 4. In many of these cases the magnitudes of the real or imaginary parts of  $Z_{CLN}$  are greater than corresponding parts of  $Z_{CJN}$ , indicating dominant compact layer effects. The Table shows that both  $Z'_{TN}$  and  $\bar{Z}_{TN}$  are quite good for  $\Omega = 10^{-2}$ ;  $Z'_{TN}$  usually remains quite adequate for the larger  $\Omega$  values; and the  $\bar{Z}_{TN}$  values are appreciably poorer for  $\Omega = 1$ . Generally, as found earlier,  $Z'_{TN}$  is a better global approximation than  $\bar{Z}_{TN}$ , but it is remarkable that they both remain as good as they do in the small  $C_{CN}$ , large  $\Omega$  region.

Quite different behavior appears for cases E and F where  $M_n \ll 1$ . Here both  $Z'_{CJN}$  and  $Z'_{CLN}$  are correct to six or more decimal places, as is  $Z'_{TN}$  as well, for all  $\Omega$  values. Although the  $\bar{Z}_{TN}$  values shown for case F in Table 4 at

TABLE 4

Exact and approximate normalized impedance results for some Table 3 cases

		$\Omega = 10^{-2}$	$\Omega = 10^{-1}$	$\Omega = 1$
C	$Z_{TN}$	10.939 - 0.8036i	7.115 - 5.116i	0.4724 - 1.582i
	$Z'_{TN}$	10.959 - 0.8196i	6.902 - 5.122i	0.4715 - 1.523i
	$\bar{Z}_{TN}$	10.939 - 0.8037i	7.111 - 5.160i	0.3671 - 1.312i
F	$Z_{TN}$	38.426 - 192.32i	0.39944 - 19.992i	$3.9960 \times 10^{-3} - 2.0000i$
	$Z'_{TN}$	38.426 - 192.32i	0.39944 - 19.992i	$3.9960 \times 10^{-3} - 2.0000i$
	$\bar{Z}_{TN}$	39.310 - 191.94i	1.3844 - 19.854i	0.50199 - 1.4980i
H	$Z_{TN}$	$2.6977 - 3.6455 \times 10^{-2}i$	2.650 - 0.3581i	0.9549 - 1.290i
	$Z'_{TN}$	$2.6977 - 3.6458 \times 10^{-2}i$	2.653 - 0.3603i	0.9151 - 1.280i
	$\bar{Z}_{TN}$	$2.6974 - 3.6450 \times 10^{-2}i$	2.622 - 0.3528i	0.7155 - 0.8087i
J	$Z_{TN}$	10.8368 - 1.3265i	4.410 - 5.357i	0.1250 - 0.8982i
	$Z'_{TN}$	10.8376 - 1.3268i	4.393 - 5.368i	0.1168 - 0.8921i
	$\bar{Z}_{TN}$	10.8374 - 1.3266i	4.404 - 5.383i	$8.406 \times 10^{-2} - 0.8921i$
K	$Z_{TN}$	6.466 - 4.995i	1.095 - 1.185i	0.4957 - 0.6023i
	$Z'_{TN}$	6.455 - 4.992i	1.090 - 1.183i	0.4962 - 0.6000i
	$\bar{Z}_{TN}$	6.473 - 5.081i	0.9058 - 1.200i	0.4408 - 0.5042i

$\Omega = 0.1$  and 1 are quite poor, one should remember that the semicircle in this case has a radius of  $1001/2$ , so all the values listed for  $\Omega = 0.1$  and 1 are very small compared to those near the middle of the semicircle, and errors in these small values are thus relatively less significant.

#### (IV) CONCLUSIONS

The results presented here and many others which have been calculated suggest that in the great majority of cases of interest, even for small  $C_{CN}$ ,  $Z'_{TN}$  is a fully adequate approximation and that in many situations even  $\bar{Z}_{TN}$  is adequate. It is worth emphasizing, however, that in the many cases where  $\bar{Z}_{TN}$  is adequate,  $\bar{C}_{RN}$  should be calculated from eqn. (13) or (14), and  $R_{RN}$  should be distinguished from  $\bar{R}_{RN}$  unless  $\nu_2 = 1$ . Only when  $C_{CN} \gg C_{DN}$  should compact layer effects be ignored and this condition is by no means satisfied in many experimental situations. The existence and wide range of adequacy of the  $\bar{Z}_{TN}$  approximation explains why relatively simple equivalent circuits, like that of Fig. 2b, have been found adequate to analyze a wide variety of ionic-conduction data. But such analyses should properly take into account the differences between  $C_{RN}$  and  $\bar{C}_{RN}$  and  $R_{RN}$  and  $\bar{R}_{RN}$  discussed herein.

Although the excellent agreement between  $Z_{TN}$ ,  $Z'_{TN}$  and  $\bar{Z}_{TN}$  for a wide range of parameter values over a wide frequency range is of primary interest, the remarkable agreement between the  $Z'_{TN}$  impedance of the circuit of Fig. 2a and the  $\bar{Z}_{TN}$  impedance of the very different and much simpler circuit of Fig. 2b with  $R_2 = \bar{R}_R$  and  $C_2 = \bar{C}_R$  is itself noteworthy. Evidently, the special relations between many of the circuit elements are instrumental in ensuring such agreement at least for  $\Omega \leq 1$  and involving a kind of similarity transformation, one where the *form* of the  $Z_{CJN}$  circuit on the left of Fig. 2a is very nearly con-

served after the series addition to it of the complicated resonant circuit on the right side of Fig. 2a.

Although  $C_C$  has been considered thus far to arise only from the finite size of charge carriers, it may in some experimental situations be influenced and even dominated by air gaps or insulating layers between the electrode and material [11–13] and/or possibly by electrode/material surface roughness effects [14,15]. In such cases, the effective  $C_C$  may be much smaller than  $C_D$ , even at the minimum of  $C_D$  at the point of zero electrode charge. The present theory still applies with such reinterpretation of  $C_C$ , and the effects of the “generalized” compact layer will dominate diffuse double layer effects and must not be ignored.

Finally, it is worth remarking that our exact treatment of systems with a compact layer [1–3] and the simplified versions presented here encompass situations ranging from the absence of compact layer effects ( $C_C \rightarrow \infty$ ), as assumed in much of the earlier work, to some of those considered by Armstrong [16] in which the diffuse layer is assumed absent ( $M \rightarrow \infty$ ). In many situations, the present results will thus be more appropriate than those obtained in either of the limiting cases.

#### ACKNOWLEDGMENTS

We appreciate programming help from Steven R. Thompson and are most grateful to the National Science Foundation for support of this work.

#### REFERENCES

- 1 D.R. Franceschetti and J.R. Macdonald, *J. Electroanal. Chem.*, **82** (1977) 271.
- 2 D.R. Franceschetti and J.R. Macdonald, *J. Electroanal. Chem.*, **87** (1978) 419. The term  $(1 - i\Omega - \nu_n)$  in eqn. (8) of this paper should be  $(1 + i\Omega - \nu_n)$ .
- 3 D.R. Franceschetti and J.R. Macdonald, *Phys. Status Solidi*, (a) **43** (1977) K169. The equation  $r_p = D_p k_p / l$  on p. K171 should be replaced by  $r_p = l k_p / D_p$ .
- 4 J.R. Macdonald and D.R. Franceschetti, *J. Chem. Phys.*, **68** (1978) 1614.
- 5 R.D. Armstrong, R.A. Burnham and P.M. Willis, *J. Electroanal. Chem.*, **67** (1976) 111.
- 6 R.D. Armstrong and W.I. Archer, *J. Electroanal. Chem.*, **87** (1978) 221.
- 7 J.R. Macdonald, *J. Chem. Phys.*, **61** (1974) 3977.
- 8 J.R. Macdonald and J.A. Garber, *J. Electrochem. Soc.*, **124** (1977) 1022.
- 9 A.A. Kornyshev and M.A. Vorotyntsev, *Phys. Status Solidi*, (a) **39** (1977) 573.
- 10 R. de Levie and K.M. Abbey, *J. Theor. Biol.*, **56** (1976) 151.
- 11 J.R. Macdonald, *J. Chem. Phys.*, **29** (1958) 1346.
- 12 J.R. Macdonald, *J. Phys. Chem. Solids*, **21** (1961) 313.
- 13 D. Miliotis and D.N. Yoon, *J. Phys. Chem. Solids*, **30** (1969) 1241.
- 14 R. de Levie, *Electrochim. Acta*, **10** (1965) 113.
- 15 D.O. Raleigh, *J. Electrochem. Soc.*, **121** (1976) 632.
- 16 R.D. Armstrong, *J. Electroanal. Chem.*, **52** (1974) 413.